

PAPER • OPEN ACCESS

# The single crystal diamond-based diagnostic suite of the JET tokamak for 14 MeV neutron counting and spectroscopy measurements in DT plasmas







To cite this article: D. Rigamonti *et al* 2024 *Nucl. Fusion* **64** 016016

View the [article online](#) for updates and enhancements.

You may also like

- [14 MeV calibration of JET neutron detectors—phase 2: in-vessel calibration](#)  
P. Batistoni, S. Popovichev, Z. Ghani et al.
- [Conceptual design of the high resolution neutron spectrometer for ITER](#)  
Marek Scholz, Anders Hjalmarsson, Leszek Hajduk et al.
- [Neutron spectroscopy measurements of tritium beam transport at JET](#)  
M. Nocente, M. Albergante, J. Eriksson et al.

# The single crystal diamond-based diagnostic suite of the JET tokamak for 14 MeV neutron counting and spectroscopy measurements in DT plasmas

D. Rigamonti<sup>1</sup> , A. Dal Molin<sup>1,\*</sup> , A. Muraro<sup>1</sup>, M. Rebai<sup>1</sup>, L. Giacomelli<sup>5</sup>, G. Gorini<sup>1,2</sup>, M. Nocente<sup>1,2</sup> , E. Perelli Cippo<sup>1</sup>, S. Conroy<sup>3</sup>, G. Ericsson<sup>3</sup>, J. Eriksson<sup>3</sup> , V. Kiptily<sup>4</sup> , Z. Ghani<sup>4</sup>, Ž. Štancar<sup>4</sup> , M. Tardocchi<sup>1</sup> and JET Contributors<sup>a</sup>

<sup>1</sup> Institute for Plasma Science and Technology, National Research Council of Italy, Milan, Italy

<sup>2</sup> Department of Physics, University of Milano-Bicocca, Milan, Italy

<sup>3</sup> Department of Physics and Astronomy, Uppsala University, Ångström laboratoriet, Lägerhyddsvägen 1, Box 516, 75120 Uppsala, Sweden

<sup>4</sup> Culham Centre for Fusion Energy, Abingdon, United Kingdom of Great Britain and Northern Ireland

<sup>5</sup> European Commission, Joint Research Centre, Ispra, Italy

E-mail: [andrea.dalmolin@istp.cnr.it](mailto:andrea.dalmolin@istp.cnr.it)

Received 18 July 2023, revised 5 October 2023

Accepted for publication 7 November 2023

Published 23 November 2023



## Abstract

The Joint European Torus (JET) has recently conducted its second deuterium–tritium (DT) experimental campaign DTE2, providing unique opportunity for studying both physics and engineering aspects of nuclear fusion plasmas. This also allowed the exploitation of new diagnostics and technologies that were not available during the first JET DT campaign held in 1997. Among these new instruments, the enhancement projects of the JET nuclear diagnostics lead to the development and installation of synthetic single crystal diamond detectors along different collimated line of sights. This paper describes the single crystal diamond-based diagnostic suite of the JET tokamak and the enhanced 14 MeV neutron diagnostic capabilities in terms of neutron yield and high resolution neutron spectroscopy. The diamond characterization measurements and the calibration procedure at JET are shown, together with performance of the diamond based neutron spectrometer as 14 MeV neutron yield monitor which allows the separation of 2.5 MeV and 14 MeV neutrons in trace tritium plasmas. The first high-resolution 14 MeV neutron spectroscopy measurements in neutral beam injection-heated DT plasmas are presented, allowing thermal and non-thermal neutron component separation. Prospects for the diagnose of DT burning plasmas such as ITER and SPARC will be presented.

<sup>a</sup> See Mailloux *et al* 2022 (<https://doi.org/10.1088/1741-4326/ac47b4>) for JET Contributors.

\* Author to whom any correspondence should be addressed.



Original content from this work may be used under the terms of the [Creative Commons Attribution 4.0 licence](https://creativecommons.org/licenses/by/4.0/). Any further distribution of this work must maintain attribution to the author(s) and the title of the work, journal citation and DOI.

**Keywords:** nuclear diagnostics, neutron spectroscopy, single crystal diamond detectors, tokamaks, nuclear fusion diagnostics

(Some figures may appear in colour only in the online journal)

## 1. Introduction

The Joint European Torus (JET) is the largest tokamak in the world and is the only one able to operate with tritium [1]. Recently, the second deuterium–tritium (DT) experimental campaign, namely DTE2, has been successfully performed giving the unique opportunity to study both physics and engineering aspects of nuclear fusion plasmas [2]. This was allowed by the exploitation of new technologies that were not available during the first DT JET campaign held in 1997. In the last ten-years, the EUROfusion enhancement projects allowed to significantly improve the diagnostics capability of JET [3–5]. In particular, significant efforts have been made to upgrade the nuclear diagnostics by developing new dedicated instrumentation able to cope with DT plasmas. Among these, a set of compact high-resolution diamond detectors has been installed at JET, enabling neutron spectroscopy measurements along different lines of sight. Neutron emission spectroscopy (NES) is a diagnostic technique based on the measurement of the neutron energy spectrum emitted along a collimated line of sight (LoS). Neutrons are directly emitted by nuclear fusion reactions carrying information on the fuel ions. Their measurement provides quantitative information on the fuel ion energy distributions integrated along the full field of view of the detector [6–8]. In case of thermal plasma, the neutron emission is isotropic and the energy distribution is well approximated by a Gaussian, with a thermal Doppler broadening that depends on the ion temperature ( $T_i$ ) via the simple relationship:  $\text{FWHM} = 82.6\sqrt{T_i}$  for DD plasmas and  $\text{FWHM} = 177.2\sqrt{T_i}$  for DT plasmas where the FWHM is the full width at half maximum of the peak [6]. From the instrumental point of view,  $T_i$  measurements are enabled when the resolution of the spectrometer matches the thermal broadening of the plasma [7]. For 2 keV thermal plasmas, the required energy resolution is at least of the order of 1.8%, which poses strict requirements on the development of the instrument. For non-Maxwellian plasmas, namely when external heating systems are applied, the simple relationship connecting the ion temperature and the thermal broadening is not valid anymore. When neutral beam injection (NBI) or ion-cyclotron radiofrequency are used, the fuel ion velocity distribution is not isotropic, resulting in a neutron energy spectrum with supra-thermal components. The supra-thermal components depend on the viewing angle subtended by the spectrometer [6] and their prediction requires the use of a proper model of the fuel ion velocity distribution and Monte Carlo techniques. High resolution neutron spectrometers allow to identify and separate the thermal and non-thermal plasma neutron components, to measure the ion temperature and to estimate the fuel ion ratio  $nT/nD$  [7]. The state of the art 14 MeV neutron spectrometer

at JET is the magnetic proton recoil (MPR) [9]. It is based on the proton recoil technique through elastic scattering of collimated neutrons on hydrogen nuclei occurring in a thin converter foil ( $\text{CH}_2$ ). The recoiled protons are then momentum selected via magnetic fields and recorded by a scintillator array plate [9, 10]. The MPR has been the reference 14 MeV neutron spectrometer during the first DT campaign in 1997. Because of its bulky volume and operational complexity, its integration in high performance tokamaks may be not straightforward. In this context, single crystal diamond detectors can represent an alternative technology for NES measurements combining compactness and high resolution. Furthermore, diamond detectors are suitable to be installed on a multi-lines of sight camera providing spectroscopy and tomography information.

While neutron spectroscopy aims at investigating the origin of the fusion reactions (e.g. thermal vs non-thermal) and the properties of the fuel ions distribution functions, absolute neutron counting provides the total number of reactions occurred in a plasma discharge. This quantity is an essential tool for the operation of fusion reactors. The neutron yield is a direct measurement of the fusion power, which is, ultimately, the goal of fusion research. At JET, the neutron yield is routinely provided by the fission chambers (FCs) and the activation foils system (AFS) diagnostics. The AFS is able to separate the 2.5 MeV and 14 MeV neutron contribution by exploiting the use of reaction channels with defined neutron energy thresholds. The measurement provides the integrated neutron yield over the whole duration of the plasma discharge. The FC, instead are used to monitor the time trace of the neutron yield. At JET, there are three pairs of ion chambers with  $^{235}\text{U}$  and  $^{238}\text{U}$  and they are placed in three different position around the tokamak in the mid-plane [11]. The FC are surrounded by a moderator material to thermalize the neutrons before reaching the active part of the detector. Due to the moderation process, the information on the neutron energy is lost, resulting in the inability to distinguish direct and scattered neutrons. Intensive Monte Carlo codes need to be run to determine the fraction of scattered/direct neutrons in order to apply a correction coefficient to the measurements. This ratio strictly depends on the materials and geometry surrounding the JET tokamak and new simulations are needed when significant modifications in the Torus Hall or inside JET are made. Furthermore, the flat response of the FC to neutrons of different energies makes it impossible to discriminate of 2.5 MeV and 14 MeV neutrons [12]. When the presence of 2.5 MeV neutrons is significant, such as in DT plasmas with low tritium concentration (less than 3%), the FC shows to be unreliable to determine the 14 MeV neutron yield. For this reason, since the first DT campaign, silicon detectors have been used

as 14 MeV neutron counters by exploiting the  $^{28}\text{Si}(n,p)^{28}\text{Al}$  and  $^{28}\text{Si}(n,\alpha)^{25}\text{Mg}$  nuclear reactions that may occur when a neutron with energy higher than 7 MeV interacts with Si nuclei [13]. In this situation, single crystal diamond detectors can play a major role. Similar to silicon based detectors, diamonds can exploit nuclear reaction channels which open up at high neutron energy thresholds. Unlike silicon detectors, diamonds have 100 times more radiation resistance [14], showing stable performances up to  $10^{14}$  n cm $^{-2}$  with 14 MeV neutrons [15].

The present paper presents the first 14 MeV neutron spectra measured at JET with synthetic diamond detectors in NBI-heated DT plasmas, and their data analysis. The analysis model considers both the thermal and the supra-thermal components which have been calculated with TRANSP and GENESIS simulations. Furthermore, the paper describes the principles of 14 MeV neutron counting with diamond detectors, with example of data from the DTE2 campaign.

## 2. Single crystal diamond detectors

The use of single crystal diamond detectors as neutron spectrometers for fusion plasma experiments started in 1997 when A. Krasilnikov measured for the first time the DT neutron spectrum with natural diamonds at JET [16] and at TFTR [17]. In the last twenty-years, significant progresses have been made in growing synthetic crystals to overcome some limitations of natural diamonds. Natural diamonds required for radiation detection purposes are of high electronic quality and, in general, their performances depends on the quantity of impurities and defects inside the crystal [18]. Since natural diamonds are not standardized items, their use on large scale was not practical and this called for artificial diamonds. So far, the best production technique is the chemical vapor deposition (CVD) which can grow electronic grade single crystal diamonds detectors [19], suitable for radiation detection purposes.

The ionizing radiation inside a diamond detector produces free electrons-holes pairs inside the active volume of the crystal. The charge carriers move toward the ohmic contacts thanks to an applied electric field, resulting in an electric pulse. The charge associated to the electric pulse represents the number of collected electron-hole pairs which is proportional to the energy deposited by the radiation inside the diamond. The neutron detection is made possible by exploiting the nuclear reactions occurring between the neutrons and the carbon nuclei inside the crystal (see figure 1). Here the electron-hole pairs are generated by the charged particles produced via neutron-induced nuclear reactions. For 14 MeV neutrons, the main reaction channels are:

- the elastic and inelastic scattering  $^{12}\text{C}(n,n')^{12}\text{C}$ , giving a flat contribution to the measured energy spectrum, with maximum energy deposition less than 4 MeV;

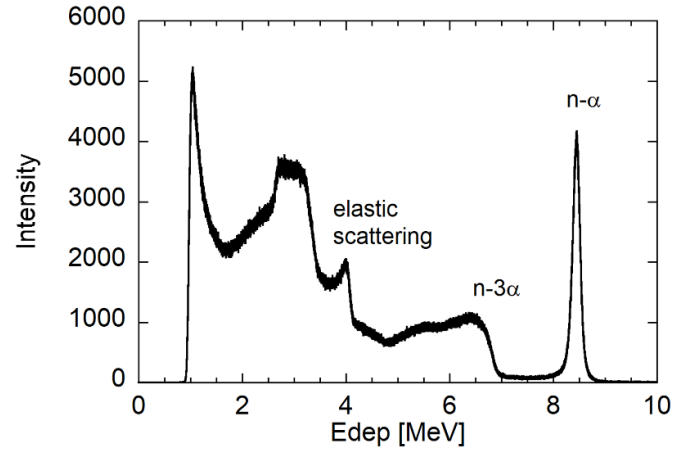


**Figure 1.** Diamond response function to 14 MeV neutron irradiation performed at the Frascati Neutron Generator (FNG-ENEA).

- the  $^{12}\text{C}(n,n')3\alpha$  with a negative  $Q_{\text{value}} = -7.23$  MeV, producing an ‘edge’ in the spectrum, with maximum energy deposition less than 7 MeV;
- the  $^{12}\text{C}(n,\alpha)^9\text{Be}$  with a negative  $Q_{\text{value}} = -5.702$  MeV, giving a Gaussian peak in the spectrum at roughly 8.3 MeV. This energy region is not affected by other reaction channels contributions.

The latter reaction is the best candidate for high resolution 14 MeV neutron spectroscopy measurements. It leads to a peak centered at the energy of the incoming neutrons plus the  $Q_{\text{value}}$  of the reaction. The analysis of this peak provides information on the 14 MeV neutron spectrum. The peak shape, in fact, comprises two contributions: the energy resolution of the detector ( $\approx 120$  keV) and the additional kinematic broadening of the energy distribution of the incoming neutrons. This method has been successfully exploited in [20] when synthetic diamonds with unprecedented energy resolution allowed to resolve for the first time the different neutron components contributing to the peak, and to estimate the beam ion composition of a 14 MeV neutron generator. The measurement and the related data analysis validated the excellent spectroscopy performances of diamonds in preparation of the DTE2 JET campaign.

The energy resolution is not the only parameter to take into account when developing a nuclear diagnostic for fusion plasma applications. Diamonds, in fact, are radiation hard instruments [14, 15], reliable and able to operate at room temperature. In addition, they are very fast (typical pulse length  $\approx 30$  ns), allowing to follow the plasma evolution with a time resolution better than 100 ms (when the neutron flux allows it) and with limited pile-up contribution. Diamond detectors can also be used to detect 2.5 MeV neutrons emitted by deuterium plasmas. Here, the only reaction allowed is the elastic scattering on  $^{12}\text{C}$  nuclei. The energy transferred to the recoiled  $^{12}\text{C}$  nuclei is determined by the scattering law

$E_{12c} = 0.284 \cdot E_n \cdot \cos \theta_R^2$  and depends on the incoming neutron kinetic energy ( $E_n$ ) and on the  $^{12}\text{C}$  recoiling angle ( $\theta_R$ ) in the laboratory coordinate system. The  $^{12}\text{C}$  recoil nuclei are fully stopped inside the crystal, resulting in a continuum in the deposited energy spectrum from zero to a maximum value which is obtained with  $\theta_R = 90^\circ$  and it is  $\approx 0.71$  MeV in case of 2.5 MeV neutron. This results in a clear separation between 2.5 MeV and 14 MeV neutrons when a threshold higher than 2 MeV (conservatively) is applied.

### 3. Characterization measurements at nuclear facilities

The diamond detectors have been calibrated and characterized before their installation at JET in order to measure their response function and energy resolution. First, alpha particle measurements have been performed in laboratory. The detectors were irradiated with a 3-alpha source (Pu-239, Am-241, Cm-244) inside a vacuum chamber to reduce the alpha particles energy straggling. A FWHM of about 96 keV has been estimated for  $E_\alpha = 5.486$  MeV, giving an energy resolution  $R = \text{FWHM}/E_\alpha = 1.74\%$  [21]. Neutron irradiation, instead, has been performed at nuclear facilities using quasi-monoenergetic neutron beams. In particular, the detector response function (see in figure 1 the example of diamond response to 14 MeV neutrons) has been measured at the Frascati Neutron Generator (FNG-ENEA), at the Peking University van de Graaff neutron source and at the CN facility at the INFN-LNL in the energy range 2.5–5.5 MeV and 14–20 MeV. Neutrons were produced via nuclear reactions between an accelerated ion beam interacting with a solid target. In particular, the exploited nuclear reactions are:

- $\text{T(d,n)}^4\text{He}$  where the deuterons were accelerated up to 270 keV or 3.3 MeV on a T-Ti target;
- $\text{T(p,n)}^3\text{He}$  and  $^7\text{Li(p,n)}^7\text{Be}$ .

The broadening of the  $\text{n-}\alpha$  peak resulted to be mainly due to the Doppler width of the neutron beam (see figure 2). For each nuclear reaction, the incoming neutron energy distribution has been calculated with the TARGET code [22] by modeling the target, in terms of materials and geometry, and the beam-target reaction. The obtained neutron energy distributions are significantly affected by the energy loss of the ions beam inside the solid target and the geometrical parameters of the experimental setup, such as the angle between the detector and the accelerated ion beam. Figure 2 shows the  $\text{n-}\alpha$  peak recorded when the diamond is irradiated with 20 MeV (top) and 15 MeV (bottom) neutrons, respectively. The black dots are the measured data, the dash line represents the calculated neutron energy distribution, while the solid line is the calculated neutron energy distribution convolved with the detector response function in the  $\text{n-}\alpha$  peak, which is a Gaussian distribution. The FWHM of the Gaussian distribution represents the finite energy resolution of the detector and resulted to be

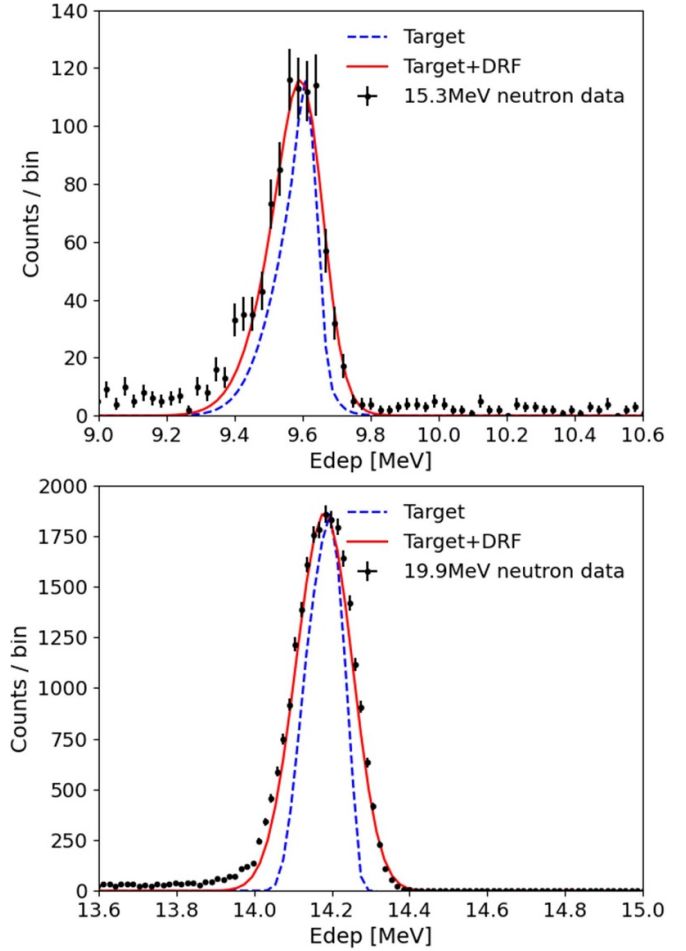


**Figure 2.** Energy spectra measured by the diamond under 19.9 MeV (top) and 15.3 MeV (bottom) neutron irradiation. Black dots are the measured data, the blue dashed line is the expected neutron distribution calculated with TARGET plus the reaction  $Q_{\text{value}}$  ( $\approx -5.7$  MeV), while the red solid line is the calculated neutron distribution convolved with the detector response function (DRF).

120–130 keV. The obtained energy resolution does not depend on the energy of the neutrons, indicating that the main contribution to the resolution comes from the electronic noise of the preamplifiers [23]. More details of all the characterization measurements at nuclear facilities are given in [21, 23, 24].

### 4. Experimental setup at JET

At JET, three diamond detectors with spectroscopic capabilities have been installed on three different LoSs (see figure 3). The first one is a  $4 \times 3$  diamonds matrix, named KM14, based on 12 independent single crystal diamonds (see figure 4) [25]. It is placed on the vertical LoS sharing the same LoS with the time-of-flight neutron spectrometer optimized for high count rate measurements [26], the reference spectrometer for 2.5 MeV neutrons. The choice to have a diamond matrix with more pixels is to boost the detection efficiency and so the counting statistics of the diagnostic, since it is far away



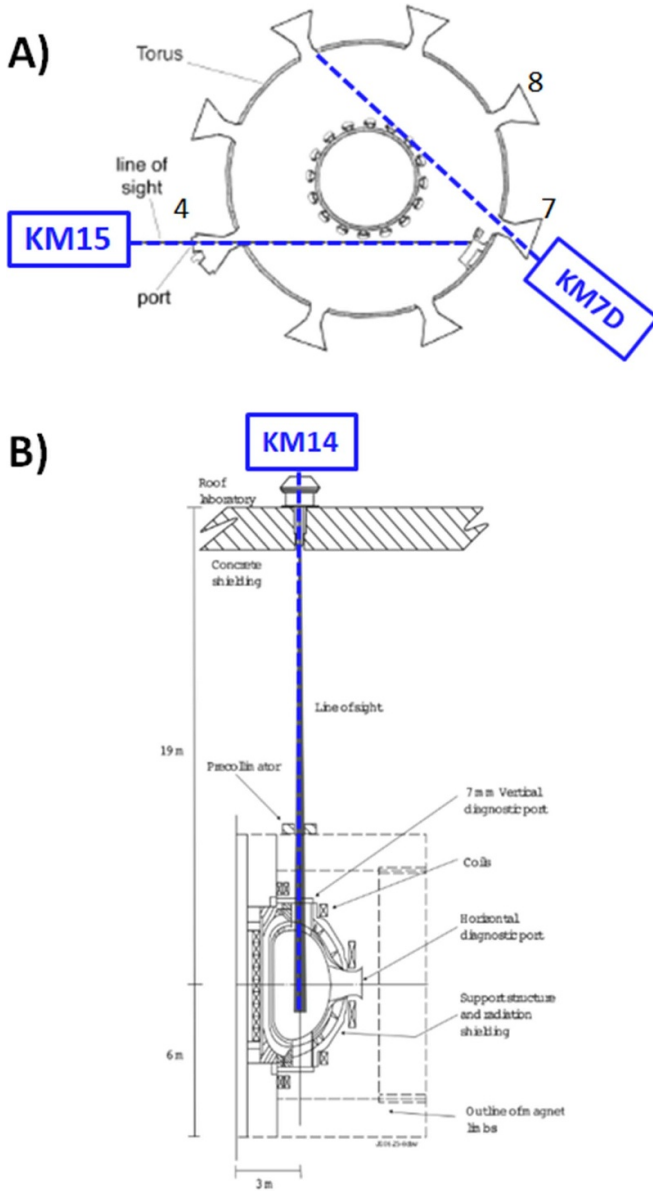


**Figure 3.** Schematic of the three lines of sight of the diamond detectors installed at JET. Figure (A) shows the tokamak from the top. Figure (B) shows the tokamak and the LoS on the poloidal plane.

from the plasma (about 20 m). The remaining two diamonds, namely KM15 and KM7D, are single pixel crystal diamond detectors installed tangentially and viewing the plasma at  $46^\circ$  and  $52^\circ$ , respectively [27, 28]. KM15 shares the same LoS of the MPR spectrometer, while KM7D is deployed in the same LoS of the tandem annular-radiator proton-recoil spectrometer (KM2) [28] and the liquid scintillator (KM12) [29]. Picture of a single crystal diamond detector is shown in figure 5. The diamond detectors are made by electron grade diamond samples grown via CVD by the Element Six Ltd [30]. The ohmic contacts on the top and bottom surfaces have been provided by CNR-ISM institute in Rome. They have been obtained via

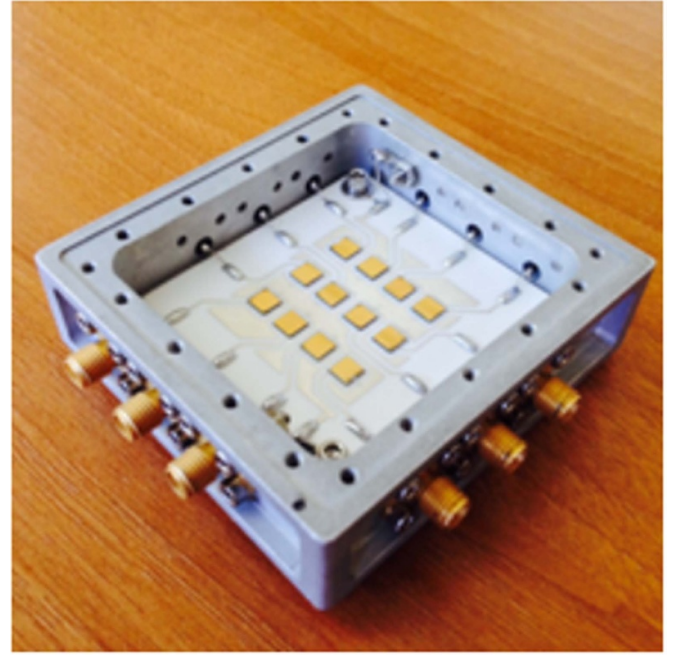


**Figure 4.** Picture of the diamond matrix installed in the vertical line of sight at JET.

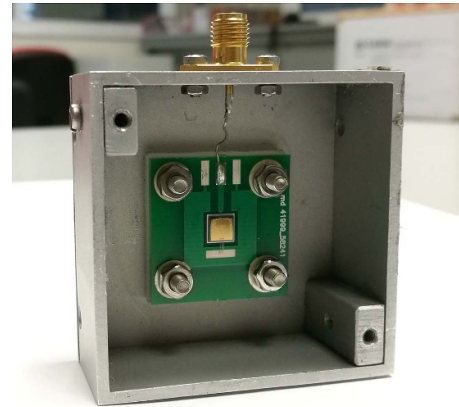


**Figure 5.** Picture of a single crystal diamond detector.

sputtering deposition of a multilayer metal structure and then finished with a gold layer deposition. Finally, the diamonds are leaning on a dedicated 1 mm thick alumina printed circuit board and protected by a metal case working as Faraday shield. The electronic chain of the three diamond based diagnostics exploits the same technology (see figure 6). The output signal is fed into a fast charge preamplifier CIVIDEC C6 [31] and then, by using a fan-in fan-out module, it is split in two channels optimized for DT and D neutrons, respectively. The first one goes directly into a 14 bits-500 Msp/s CAEN digitizer DT5730 [32] while the second channel is further amplified by using a CIVIDEC C1 and then digitized. The CAEN digitizer is provided with a dedicated firmware able to perform online analysis in order to reduce the amount of data to store. For each

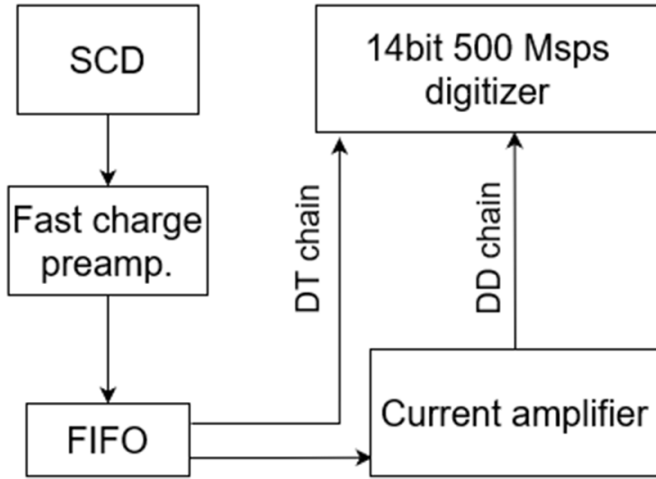


**Figure 6.** Schematic of the electronic chain.

event, the digitizer provides the timestamp and the integral of the signals under two selectable gates. The integral is proportional to the energy deposited by the neutron inside the diamond and is used to produce the energy deposited spectrum. The gain stability of the diamonds is continuously monitored with a 3-alpha source (Pu-239, Am-241, Cm-244) placed in front of the detector (figure 7). The alpha spectra are recorded before and after each JET discharge for 40 s, which are enough to collect a suitable counting statistics. The idea to have the same technology looking at the plasma with different angles with respect to the toroidal magnetic field, allows to investigate the anisotropy of the fuel ion distribution function which is due to the use of the external heating systems. The vertical LoS better highlights the features due to the radio frequency heating, while the tangential one highlights the features of the beams. Furthermore, the three diagnostics are placed at different distances with respect to the JET plasma allowing to cover the whole neutron yield range of JET ( $10^{16}$ – $10^{19}$  n s $^{-1}$ ). For this paper, a few JET plasma discharges with D and T NBI heating systems have been considered and analyzed.

#### 4.1. Calibration and characterization method at JET

The diamond detectors have been calibrated and characterized *in-situ* at JET by using both the tri-alpha particles sources (see figure 7) and the 14 MeV neutron peak measured during the ohmic phases of DT plasmas (see figure 8). The latter can be used as calibration point since the neutron emission in ohmic plasma is isotropic and its energy is well known and it does not depend on the angle of the LoS at which the neutrons are detected. The ohmic plasmas at JET are characterized by a low neutron yield, typically less than  $1 \times 10^{13}$  n s $^{-1}$ . In order to have a reasonable counting statistic in the peak, the neutron spectra related to the ohmic phases of 44 JET plasma discharges (from 99 304 to 99 347) have been summed together, after the one to one gain correction with alpha sources. The calibration resulted to be extremely linear (see figure 9). The calibration point related to the 14 MeV neutron peak (blue square in

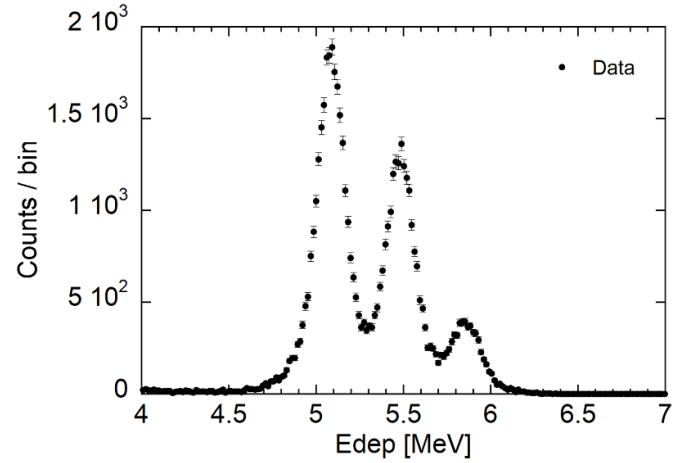


**Figure 7.** Example of energy spectrum measured by the diamond detector at JET when exposed to a 3-alpha calibration source.

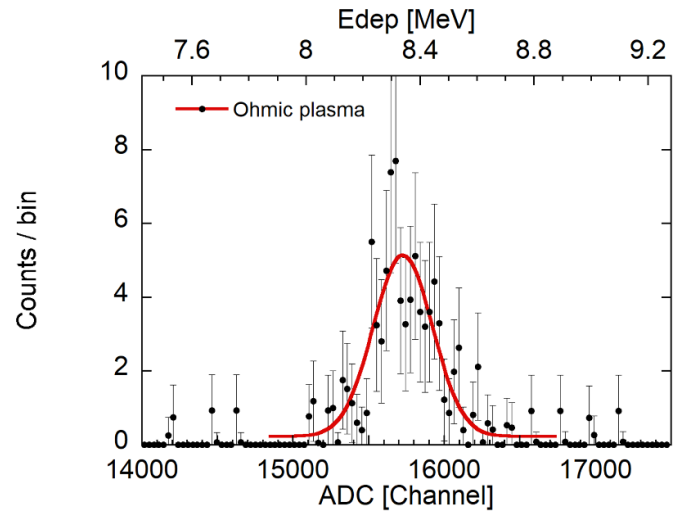


**Figure 8.** Example of 14 MeV neutron peak measured by the diamond in ohmic DT plasmas at JET. Data come from summing 44 discharges. X-axis in the bottom are the non-calibrated channels from the digitizer, x-axis in the top represents the energy deposited in MeV inside the diamond.

figure 8), which translates in  $\approx 8.3$  MeV of energy deposited, perfectly leans on the line even when it is not included in the fit. The remaining calibration points are related to the tri-alpha source and their difference in energy. The tri-alpha source has also been used to cross check the detectors performances after their installation at JET. A Monte Carlo simulation with MCNP code has been performed to calculate the deposited energy spectra of the alpha particles inside the diamonds, taking into account their straggling in air before reaching the detectors. Then the simulated spectra have been convolved with a Gaussian function, whose width (FWHM) represents the finite energy resolution of the detector, and then fitted to the measured data. The lowest reduced Chi square has been obtained by using an energy resolution of 125 keV, in terms of FWHM. This confirmed the value found at the nuclear facilities (see section 3).

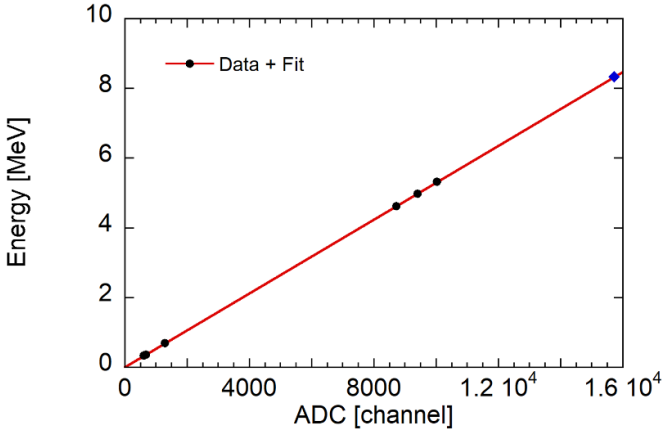


**Figure 9.** Example of calibration line obtained with the tri-alpha source (black dots) and the 14 MeV neutron peak (blue square) with ohmic DT plasmas.

## 5. First experimental results and data analysis on JET DT plasmas

In this section, first results achieved during the DTE2 on 14 MeV neutron measurements with diamond detectors will be presented. The first part will report the 14 MeV neutron yield measurements. In this context, diamond detectors are an essential tool for monitoring the 14 MeV neutron production which are of particular interest at low tritium concentration in DT plasmas. Diamonds, in fact, can operate with no limitations related to the D or T concentration as they provide spectral separation of 2.5 MeV and 14 MeV neutrons. The second part will be dedicated on high resolution spectroscopy measurements showing the capability to resolve the different neutron components in order to measure the thermal/non-thermal fraction, to isolate the thermal component and to infer back the ion temperature.

### 5.1. DT neutron yield measurements in DT plasmas

As demonstrated in [33], diamond detectors are reliable instruments for neutron counting on tokamaks. Unlike the diamonds used in [33], where their design was optimized for counting 2.5 MeV neutrons by exploiting a deposited layer of Li on the diamond surface, this paper is focused on the intrinsic capability of single crystal diamond detectors to separate 2.5 MeV and 14 MeV neutrons. Since the diamond detectors installed at JET are not absolutely calibrated, the counts measured by the diamonds have been compared to the JET FC data. Then, a calibration factor has been estimated to convert from measured counts to neutron yield. Due to a significant difference in term of maximum energy deposited inside the diamond for 2.5 MeV and 14 MeV neutrons, that is about 0.7 and 8.3 MeV respectively, a simple energy threshold can be used to count only DT neutrons. For this purpose, the number of events under the n- $\alpha$  peak have been used for counting the 14 MeV neutrons. This also provides a net separation between direct and scattered neutrons which, under the peak, can be at the level of

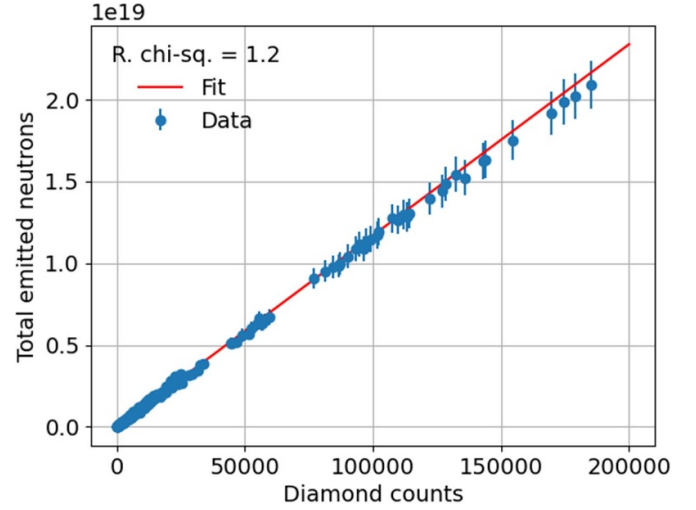


**Figure 10.** Correlation between the diamond counts and the integrated total neutron yield measured by the fission chambers in plasma discharges with tritium percentage higher than 10%.

a few percent ( $\approx 3\%$ ). Thanks to the alpha calibration measurements performed before and after each JET shot, the counting threshold was ad hoc corrected taking into account the gain shift of the detector. More than 200 JET plasma discharges in wide dynamic range from about  $5 \times 10^{15}$  to  $2 \times 10^{19}$  total JET neutrons were selected for the analysis. A linear correlation (see figure 10) with the FCs has been found in DT plasmas with tritium percentage higher than 10%. The error on the value of the total emitted neutrons is 7%, as provided by JET, while the errors on the diamond counts is the square root of the counts. It has been found that the total neutron emission provided by the FCs in low tritium discharges ( $T < 3\%$ ) is affected also by the contribution due to the 2.5 MeV neutrons (see figure 11). At low tritium discharges the DD fusion reactions are significant and the total neutron emission cannot be ascribed only to 14 MeV neutrons.

### 5.2. High resolution 14 MeV neutron spectroscopy measurements at JET

From the analysis of the measured neutron energy spectrum, different information on the plasma parameters can be inferred. In the following analysis, only the n- $\alpha$  peak will be considered, because it is an accurate representation of the incoming neutron energy spectrum. The peak position is defined by the average energy of the incoming neutrons. A Doppler energy shift  $\Delta E = c \cdot \cos \vartheta \cdot v_{rot}$  produced by the plasma rotation can appear [34]. It depends on the emission angle ( $\vartheta$ ) of the neutrons (defined by the LoS), the plasma rotational velocity ( $v_{rot}$ ) and a  $c$  coefficient related to the interested fuel ion population (and it is equal to 0.542 for the bulk emission component, 0.217 for the NBI<sub>D</sub> on T bulk and 0.325 for the NBI<sub>T</sub> on D bulk [35]). Finally, the measured neutron peak consists of multiple neutron components which are generated by different fuel ion populations characterized by different velocity distributions, such as the thermal one, the beam-thermal and the beam-beam (BB) component. The thermal



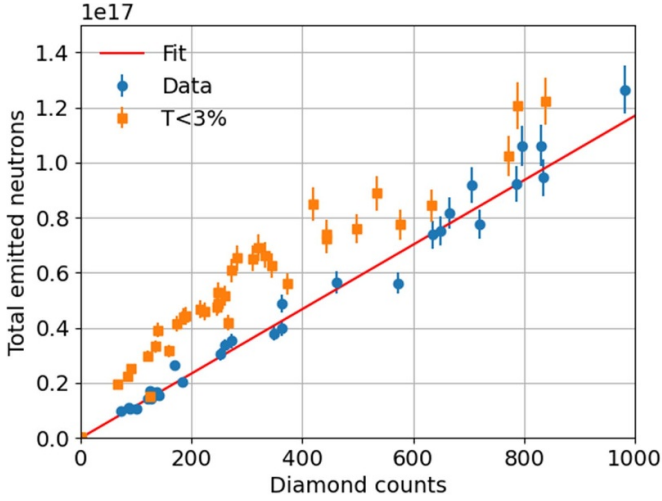


**Figure 11.** Total neutron yield measured by the fission chambers (y-axis) vs the counts of the diamond detector related to 14 MeV neutrons. Orange squares refers to JET plasma discharges with  $T < 3\%$  which are not in agreement with the correlation line found in high tritium plasma discharges.

neutron component is generated by the fusion reactions of the two fuel ions (DT) from the bulk thermal distribution. It is known that the neutron spectrum emitted by ohmic plasma is well described by a Gaussian distribution so that the DT fuel ion distributions are assumed to be in thermal equilibrium with a temperature  $T_i$  [36]. Example of neutron spectrum emitted from thermal plasmas is shown in figure 8, in which the ohmic phases of 44 JET plasma discharges (from 99 304 to 99 347) have been summed together. Here, the width of the neutron peak is a measurement of the ion temperature which resulted to be about 2.3 keV with an energy Doppler shift of  $\approx 13$  keV corresponding to a rotational velocity of  $35 \text{ km s}^{-1}$  [36]. Previous measurements of the ohmic ion temperature at JET performed with neutron spectroscopy during the first DT campaign in 1997, provided values between 2 and 3 keV which are in line with the one found with diamonds [37–39]. The beam-thermal component, instead, is produced by the ions from a thermal distribution interacting with the ion population from the neutral beam slowing-down distribution. Finally, the BB neutron component is generated by the fusion reaction of the ions resulting from the neutral beam slowing-down distributions [7, 34, 37]. In this context, in case of plasmas heated by external heating systems, high resolution neutron spectroscopy measurements allow to identify and resolve the different neutron emission components and to extrapolate the thermal/non-thermal ratio, which is a crucial parameter for high power performance tokamaks. Here, the analysis is based on the numerical fit of the measured data with the expected neutron components. The model relies on the fuel ion velocity distributions simulated by TRANSP [37, 40, 41]. The interpretive TRANSP simulations have been performed using validated fits of the electron density and temperature, ion temperature, in addition to a prescribed D–T composition based on measurements of the residual gas analysis diagnostic, as described in detail in [42]. The resulting fuel ion

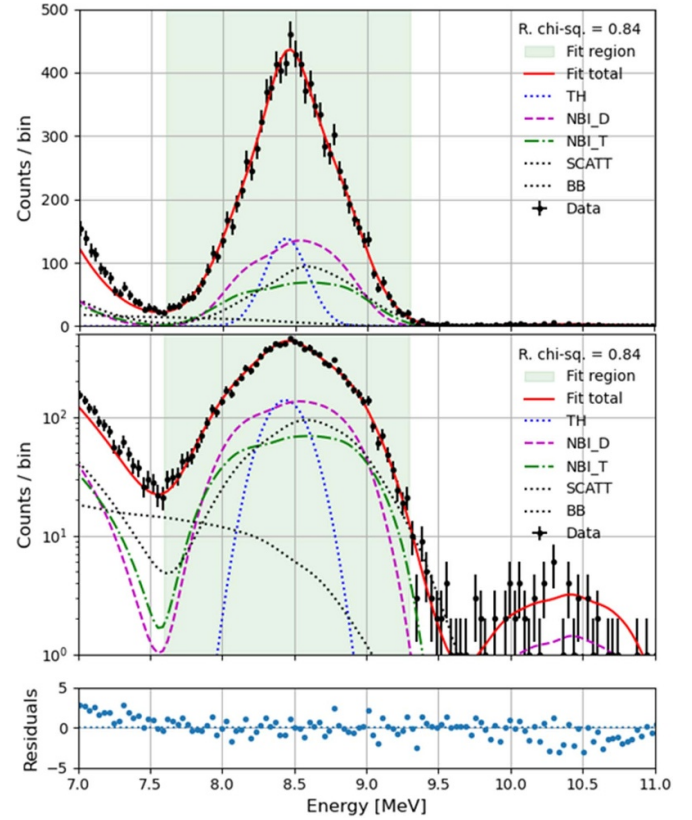


**Figure 12.** Energy spectrum measured in JET pulse number (JPN) 99346 by the oblique diamond detector in linear (top) and logarithmic (bottom) scale, together with the best numerical fit and the calculated neutron components. The TH component represents the thermal one. The NBI\_D and NBI\_T components represent the beam-thermal component of D and T beam ions interacting with the T and D thermal distributions, respectively. The BB neutron component is the beam-beam one, while the SCATT component is the scattered one. On the bottom, the distribution of the normalized residuals is shown.

velocity distributions have been used as input for calculating the expected neutron components. To do this, a Monte Carlo code named GENESIS [43–45] has been exploited simulating the neutron components integrated along the full LoS of the selected instrument. Figure 12 shows the neutron spectrum measured in JET pulse number (JPN) 99346 by the tangential diamond detector, together with the full analysis model. An overview of the main plasma parameters of the JPN99346 discharge are shown in figure 13. The neutron rate is the one measured by the FCs, the electron density is a line averaged measurement performed by the High Resolution Thomson Scattering diagnostic, providing also the electron temperature ( $T_e$ ) on magnetic axis. Finally, the ion temperature ( $T_i$ ) is measured by the charge exchange diagnostic. The green region in figure 12 represents the energy interval used for the fit while the red line is the numerical fit that overlaps the measured data (black dots). A reduced chi square lower than 1 has been found highlighting the goodness of the fit. The numerical neutron components have been used for the analysis in terms of spectral shape, while their intensity is the output result of the numerical fit (see table 1). The analysis revealed a

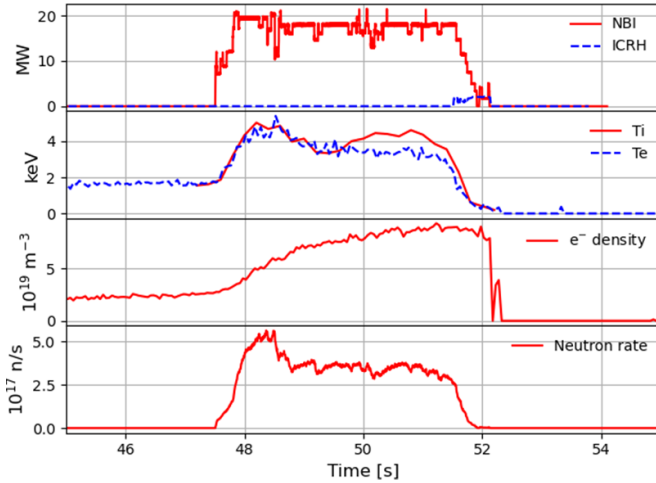


**Figure 13.** Overview of the main plasma parameters of the JPN99346 discharge.

**Table 1.** Table of the neutron components.

Neutron component	Intensity %
Thermal	$17 \pm 4$
NBI_D	$32 \pm 8$
NBI_T	$23 \pm 10$
Beam-beam	$24 \pm 13$
Scattered	$3.7 \pm 1.4$

thermal/non-thermal neutron emission fraction of the order of 21%, which is a crucial parameter for high power performance tokamaks. In this particular JET plasma discharge, both deuterium (NBI\_D) and tritium (NBI\_T) beams were injected. This resulted in a third neutron component, namely BB (in figure 12), generated by the fusion reactions of the beam ions themselves. These three components are quite similar in terms of mean energy and spectral shape, producing a significant statistical error when their intensity is inferred with the numerical fit. The thermal component has been fitted using the ion temperature both as a predefined input and as a free parameter. No significant differences have been achieved with the two approaches, resulting in a line integrated ion temperature of about  $3.5 \pm 1$  keV, in agreement with the value provided by the JET charge exchange diagnostic. The measured spectrum shows an almost flat contribution ending at 9 MeV which represents the neutrons losing their energy via scattering reactions before reaching the spectrometer. This contribution resulted to be of the order of a few percent with respect to the total neutrons. A structure in the energy range 10–10.5 MeV appears at level of 2 order of magnitude less with respect to the main peak. It is due to the  $n-\alpha$  reaction on the isotope  $^{13}\text{C}$  and is a nuisance contribution in case of investigation of high energy tails of low intensity, such as the alpha knock-on. A total energy shift of  $93 \pm 10$  keV has been found for the main neutron peak, revealing a plasma rotational velocity of about  $250 \text{ km s}^{-1}$  that is in disagreement with the value found by CXRS [46].

## 6. Discussion

The presented analysis highlighted the unprecedented capabilities of the diamond detector. Its enhanced energy resolution allowed for the first time with NES techniques to measure low ion temperatures of the order of a few keV in a significant non-thermal plasma. If we extrapolate this result to more favorable future scenarios in which the plasma is mainly thermal, such as on ITER and SPARC [47–50], this could open to real time monitoring of the ion temperature. So far, the measurement of the ion temperature with NES in non-thermal plasmas relies on the detailed analysis of the neutron peak that exploits the use of models based on simulations which cannot be done in real time. In a quasi thermal plasma, instead, the measurement of the ion temperature simply relies on the analysis of the Gaussian thermal distribution which is not expensive in term of computational resources and can be done online on FPGA (field programmable gate array). Here, the integral time of the measurements would be limited only by the counting statistics of the detector which, based on the experience, allows time resolutions as low as 10 ms. Time resolved measurements of neutron spectra and separation of thermal and non-thermal components as a function of time have also been possible with diamond detectors at JET. Concerning measurements of the neutron yield, a linear correlation between the integral neutron yield measured by the FCs and the counts collected by the diamonds has been demonstrated with plasmas with tritium percentage higher than 10%. It has been found that the total neutron emission provided by the FCs in low tritium discharges cannot be ascribed only to 14 MeV neutrons. At low tritium percentage, in fact, the 2.5 MeV neutron contribution is significant and depends by the deuterium quantity weighted on the DD cross section with respect to the tritium one weighted on the DT cross section. For this reason, JET shots with low tritium percentage (below 10%) were not taken into account in the fit. No neutron emission profiles and plasma positions were taken into account in the analysis. The diamond used for the analysis is the one behind the MPR and it is placed inside a oblique collimated LoS, viewing only a portion of the total plasma. The LoS passes twice through the center of the plasma and it is slightly tilted to reduce the effect of different plasma positions on the  $z$ -axis. A dedicated work will be done in order to evaluate the goodness of the LoS and to correct the effects due to different emission profiles and to decrease the spread of the data, as done for the MPR spectrometer in [51] during the first JET DT campaign in 1997.

## 7. Conclusions

The recent DT experimental campaign DTE2 conducted at JET in 2021 offered the unique opportunity to study both physics and technological aspects of nuclear fusion plasmas. In particular, it allowed for 14 MeV NES measurements with synthetic diamond detectors installed on multi-lines of sight. The measurement, together with a numerical model based on TRANSP and GENESIS simulations allowed for identifying and resolving the different plasma components, i.e.

NBI\_D, NBI\_T, BB and the thermal component. The latter is a Gaussian distribution whose broadening is representative of the ion temperature of the plasma. The limit to the measurement of low ion temperatures is given by the energy resolution of the detector that needs to be at least comparable to the thermal Doppler broadening itself. The enhanced energy resolution of diamond detectors enabled to extract the ion temperature of 3.5 KeV in a predominantly non-thermal plasma (JPN99346). When we extrapolate this result to future fusion reactors in which the neutron emission is dominated by the thermal plasma, it opens up to real time measurements of the ion temperature. This would be based on the simple analysis of the Gaussian thermal peak which can be achieved online on FPGA. The exploitation of the same instrument on two different lines of sight provides information on the anisotropy of the neutron emission. This work highlights the potential capabilities of the single crystal diamond detectors as high resolution neutron spectrometers whose compactness allows their easily integration on multi-lines of sight in the future DT fusion reactors. The use of diamond detectors as 14 MeV neutron counter for DT fusion power measurements has been demonstrated.

## Acknowledgments

This work has been carried out within the framework of the EUROfusion Consortium, funded by the European Union via the Euratom Research and Training Programme (Grant Agreement No. 101052200—EUROfusion). Views and opinions expressed are however those of the author(s) only and do not necessarily reflect those of the European Union or the European Commission. Neither the European Union nor the European Commission can be held responsible for them.

## ORCID iDs

D. Rigamonti  <https://orcid.org/0000-0003-0183-0965>  
 A. Dal Molin  <https://orcid.org/0000-0003-0471-1718>  
 M. Nocente  <https://orcid.org/0000-0003-0170-5275>  
 J. Eriksson  <https://orcid.org/0000-0002-0892-3358>  
 V. Kiptily  <https://orcid.org/0000-0002-6191-7280>  
 Ž. Štancar  <https://orcid.org/0000-0002-9608-280X>

## References

- [1] Wesson J. 1999 The science of JET *JET Joint Undertaking* p 20
- [2] Mailloux J et al 2022 *Nucl. Fusion* **62** 042026
- [3] Rigamonti D. et al 2018 *Rev. Sci. Instrum.* **89** 10I116
- [4] Rigamonti D. et al 2016 *Rev. Sci. Instrum.* **87** 11E717
- [5] Nocente M. et al 2022 *Rev. Sci. Instrum.* **93** 093520
- [6] Jarvis O.N. 1994 *Plasma Phys. Control. Fusion* **36** 209
- [7] Ericsson G. 2019 *J. Fusion Energy* **38** 330–55
- [8] Eriksson J. et al 2019 *Plasma Phys. Control. Fusion* **61** 014027
- [9] Ericsson G. et al 2001 *Rev. Sci. Instrum.* **72** 759–66
- [10] Sundén E. et al 2009 *NIM* **610** 682
- [11] Syme D.B. et al 2014 *Fusion Eng. Des.* **89** 2766–75
- [12] Jarvis O.N. et al 1992 *Rev. Sci. Instrum.* **63** 4511–6
- [13] Conroy S. 1988 *Nucl. Fusion* **28** 2127
- [14] Shimaoka T. et al 2016 *Rev. Sci. Instrum.* **87**
- [15] Pillon M., Angelone M., Aielli G., Almagiva S., Marinelli M., Milani E., Prestopino G., Tucciarone A., Verona C. and Verona-Rinati G. 2008 *J. Appl. Phys.* **104** 054513
- [16] Krasilnikov A.V., Amosov V.N., Belle P.V., Jarvis O.N. and Sadler G.J. 2002 *Nucl. Instrum. Methods Phys. Res. A* **476** 500–5
- [17] Krasilnikov A.V. et al 1997 *Rev. Sci. Instrum.* **68**
- [18] Angelone M. and Verona C. 2021 *J. Nucl. Eng.* **2** 422–70
- [19] Girolami M. et al 2015 *Phys. Status Solidi a* **212** 1–7
- [20] Rigamonti D. et al 2018 *Meas. Sci. Technol.* **29** 045502
- [21] Rigamonti D. et al 2015 Capabilities of a Diamond Detector matrix for neutron spectroscopy measurements at JET *European Conf. on Plasma Diagnostics ECPD (Frascati, Italy)* p PoS(ECPD2015)061
- [22] Schlegel D. 2005 *Target User's Manual, Laboratory Report* PTB-6.42–05-2
- [23] Rebai M. et al 2016 *Rev. Sci. Instrum.* **87** 11D823
- [24] Giacomelli L. et al 2016 *Rev. Sci. Instrum.* **87** 11D822
- [25] Muraro A. et al 2016 *Rev. Sci. Instrum.* **87** 11D833
- [26] Gatu Johnson M. et al 2008 *Nucl. Instrum. Methods Phys. Res. A* **591** 417
- [27] Cazzaniga C. et al 2014 *Rev. Sci. Instrum.* **85** 043506
- [28] Hawkes N.P., Bond D.S., Kiptily V., Jarvis O.N. and Conroy S.W. 2002 *Nucl. Instrum. Methods Phys. Res. A* **476** 490–4
- [29] Giacomelli L., Belli F., Binda F., Conroy S.W., Eriksson J., Milocco A., Popovicev S. and Syme D.B. 2018 *Rev. Sci. Instrum.* **89** 10I113
- [30] Element Six Ltd (available at: [www.e6.com](http://www.e6.com))
- [31] Cividec (available at: [www.cividec.at](http://www.cividec.at))
- [32] Caen (available at: [www.caen.it](http://www.caen.it))
- [33] Angelone M. et al 2008 *Nucl. Instrum. Methods Phys. Res. A* **595** 616–22
- [34] Henriksson H., Ballabio L., Conroy S., Ericsson G., Gorini G., Hjalmarsson A., Källne J. and Tardocchi M. 2001 *Rev. Sci. Instrum.* **72** 832–5
- [35] Bielecki J and Kurowski A 2019 *J. Fusion Energy* **38** 386–393
- [36] Jarvis O.N., Gorini G., Hone M., Källne J., Sadler G., Merlo V. and van Belle P. 1986 *Rev. Sci. Instrum.* **57** 1717
- [37] Henriksson H. et al 2005 *Plasma Phys. Control. Fusion* **47** 1763
- [38] Henriksson H. Neutron spectroscopy studies of heating effects in fusion plasmas *PhD Thesis* Acta Universitatis Upsalie
- [39] Eriksson B., Conroy S., Ericsson G., Eriksson J., Giacomelli L., Hjalmarsson A. and Weiszflog M. 2021 *Rev. Sci. Instrum.* **92** 033538
- [40] Hawryluk R.J. 1980 An empirical approach to tokamak transport *Physics of Plasmas Close to Thermonuclear Conditions* vol 1, ed B. Coppi et al (CEC) pp 19–46
- [41] TRANSP (available at: <https://transp.pppl.gov/index.html>)
- [42] Štancar Z. et al 2023 Overview of interpretive modelling of fusion performance in JET DTE2 discharges with TRANSP Submitted to Nuclear Fusion—Special Issue on JET T & DT
- [43] Tardocchi M. et al 2011 Spectral broadening of characteristic  $\gamma$ -ray emission peaks from  $^{12}\text{C}(^3\text{He}, p\gamma)^{14}\text{N}$  reactions in fusion plasmas *Phys. Rev. Lett.* **107** 205002
- [44] Nocente M. 2012 Neutron and gamma ray emission spectroscopy as fast ion diagnostics in fusion plasmas *PhD Thesis* Università di Milano-Bicocca, Milan, Italy
- [45] Rigamonti D. et al 2019 *JINST* **14** C09025
- [46] Negus C.R., Giroud C., Meigs A.G., Zastrow K.-D. and Hillis D.L. (JET-EFDA Contributors) 2006 Enhanced core

- charge exchange recombination spectroscopy system on Joint European Torus *Rev. Sci. Instrum.* **77** 10F102
- [47] ITER Organization *ITER Research Plan within the Staged Approach (Level III—Provisional Version) ITER Technical Report No. ITR-18-003*
- [48] Eriksson L.-G. *et al* 2007 *Report on the Task: ICRF, NBI and ITER Diagnostics* TW6-TPDS-DIADEV (Istituto di Fisica del Plasma “P. Caldirola”)
- [49] Greenwald M. 2020 Status of the SPARC physics basis *J. Plasma Phys.* **86** 861860501
- [50] Creely A., Greenwald M., Ballinger S., Brunner D., Canik J., Doody J. and Zhu J. 2020 Overview of the SPARC tokamak *J. Plasma Phys.* **86** 865860502
- [51] Sjöstrand H. *et al* (JET EFDA Contributors) 2010 Fusion power measurement using a combined neutron spectrometer-camera system at JET *Fusion Sci. Technol.* **57** 162–75